View metadata, citation and similar papers at core.ac.uk

brought to you by CORE

provided by Elsevier - Publisher Connector

Cell, Vol. 103, 781–792, November 22, 2000, Copyright ©2000 by Cell Press

X-Ray Structures of the Universal Translation Initiation Factor IF2/eIF5B: Conformational Changes on GDP and GTP Binding

Antonina Roll-Mecak,* Chune Cao,‡ Thomas E. Dever,‡ and Stephen K. Burley*†§

*Laboratories of Molecular Biophysics
†Howard Hughes Medical Institute
The Rockefeller University
New York, New York 10021
‡Laboratory of Eukaryotic Gene Regulation
National Institute of Child Health and Human Development
National Institutes of Health
Bethesda, Maryland 20892

Summary

X-ray structures of the universal translation initiation factor IF2/eIF5B have been determined in three states: free enzyme, inactive IF2/eIF5B·GDP, and active IF2/eIF5B·GTP. The "chalice-shaped" enzyme is a GTPase that facilitates ribosomal subunit joining and Met-tRNA$_i$ binding to ribosomes in all three kingdoms of life. The conserved core of IF2/eIF5B consists of an N-terminal G domain (I) plus an EF-Tu-type β barrel (II), followed by a novel α/β/α-sandwich (III) connected via an α helix to a second EF-Tu-type β barrel (IV). Structural comparisons reveal a molecular lever, which amplifies a modest conformational change in the Switch 2 region of the G domain induced by Mg^{2+}/GTP binding over a distance of 90 Å from the G domain active center to domain IV. Mechanisms of GTPase function and ribosome binding are discussed.

Introduction

Protein synthesis in *e*ukaryotes utilizes at least twelve distinct translation *i*nitiation *f*actors (or eIFs), only two of which are common to eubacteria and the archaea (IF2/eIF5B and IF1/eIF1A). Eukaryotic IF2/eIF5B was first identified in *Saccharomyces cerevisiae* (Choi et al., 1998). Subsequently, IF2/eIF5Bs were detected in other eukaryotes (Lee et al., 1999; Wilson et al., 1999; Carrera et al., 2000) and in various archaebacteria (Lee et al., 1999), suggesting that this conserved, monomeric G protein is central to protein synthesis in all living organisms. *Escherichia coli* IF2 is essential for viability (Laalami et al., 1991), and promotes binding of fMet-tRNA^{fMet} to the small ribosomal subunit (reviewed in Gualerzi and Pon, 1990; Wu et al., 1996) and ribosomal subunit joining (Kolakofsky et al., 1968). Although IF2/eIF5B is not required for survival of laboratory yeast strains, deletion of the *FUN12* gene dramatically impairs translation initiation both in vitro and in vivo (Choi et al., 1998). The resulting severe slow growth phenotype can be complemented by introduction of genes encoding human or archaeal homologs (Lee et al., 1999).

Like eubacterial IF2, eukaryotic IF2/eIF5Bs contribute to ribosomal subunit joining and function as GTPases that are maximally activated by the presence of both ribosomal subunits (Pestova et al., 2000). Ribosomal subunit joining, per se, must be independent of GTP hydrolysis, because nonhydrolyzable GTP analogs suffice for eukaryotic ribosome assembly (Pestova et al., 2000). As seen in other GTPases (reviewed in Kjeldgaard and Nyborg, 1992), IF2/eIF5B is thought to undergo conformational changes between its GTP- and GDP-bound states. Structural "switching" could, therefore, permit control of eukaryotic ribosome assembly. In this case, however, G protein dependent regulation does not appear to require a guanine nucleotide exchange factor (i.e., GTP and GDP affinities are comparable).

Eukaryotic IF2/eIF5Bs possess three characteristic segments, including a divergent N-terminal region followed by conserved central and C-terminal segments (Figure 1). This core region is conserved among all known eukaryotic and archaeal IF2/eIF5Bs and eubacterial IF2s (pair-wise amino acid sequence identities, 27%–53%), suggesting that they share a common three-dimensional structure (Sander and Schneider, 1991). The highest sequence conservation occurs within the G domain (pair-wise identities, 43%–70%). Site-directed mutagenesis of conserved residues implicated in GTP binding and/or hydrolysis has confirmed the functional importance of the G domain and, by inference, GTP hydrolysis in translation initiation. Such mutations inactivate IF2/eIF5B in both *E. coli* (Luchin et al., 1999) and *S. cerevisiae* (Lee et al., 1999). In yeast, the divergent N terminus of IF2/eIF5B is not required for function, and full-length archaeal IF2/eIF5Bs (consisting of core region only) from *Methanococcus jannaschii* and *Methanobacterium thermoautotrophicum* (*M. therm.*) substitute for yeast IF2/eIF5B in vivo and in vitro (Lee et al., 1999 and data not shown).

As a first step toward understanding the molecular bases for the mechanism(s) of action of this universal translation initiation factor, we have determined X-ray structures of full-length *M. therm.* IF2/eIF5B in three states: free enzyme, inactive IF2/eIF5B·GDP, and active IF2/eIF5B·GTP (using the nonhydrolyzable GTP analog guanosine-5′-(β,γ-imido) triphosphate, GDPNP). These three 2.0–2.2 Å resolution structures reveal an extended molecule with a novel domain architecture that resembles a chalice. Active site conformational differences between the GDP- and GTP-bound forms of the enzyme are amplified by an articulated lever system that transmits the effects of GTP binding over a distance of 90 Å from the G domain active site to the C terminus. A mechanism for IF2/eIF5B function is proposed, and possible interactions with other components of the translation machinery are discussed. This work represents a complete structural elucidation (free enzyme, GDP-, and GTP-bound) of a GTPase that does not require a guanine nucleotide exchange factor.

Results and Discussion

Crystallization and Structure Determination

Full-length *M. therm.* IF2/eIF5B bound to GDP yielded high-quality crystals containing one molecule/asymmet-

§To whom correspondence should be addressed (e-mail: burley@rockvax.rockefeller.edu).

ric unit (Experimental Procedures). The structure of IF2/eIF5B·GDP was determined via multiwavelength anomalous dispersion (MAD) (Hendrickson, 1991) (Table 1). Current working and free R factors (Brünger, 1992) for IF2/eIF5B·GDP refined at 2.0 Å resolution are 22.0% and 26.5%, respectively. Refinement of the isomorphous free enzyme structure was started with the structure of IF2/eIF5B·GDP (excluding GDP and residues involved in nucleotide binding). The current refinement model of free *M. therm.* IF2/eIF5B at 2.2 Å; resolution has an R-factor of 24.3% with a free R value of 27.5%. The structure of IF2/eIF5B·GDPNP was solved by molecular replacement (Experimental Procedures) using the IF2/eIF5B·GDP structure as the source of independent search models for individual protein domains. The current refinement model of the IF2/eIF5B·GDPNP complex at 2.0 Å resolution has an R factor of 23.1% and a free R value of 26.7%. For simplicity, IF2/eIF5B·GDPNP will be referred to as IF2/eIF5B·GTP throughout. (See Experimental Procedures and Table 1 for a complete description of the crystallographic structure determinations and subsequent refinements.)

Structural Overview

The ventral surface of IF2/eIF5B·GTP is illustrated in Figure 2, showing bound nucleotide and a Mg^{2+} counterion. The polypeptide chain consists of four domains arranged in the form of a molecular "chalice" (height 110 Å, maximum diameter 66 Å). Domains I–III form the cup, connecting downwards through a long α helix to domain IV, which forms the base. A similarity search using the Dali server (Holm and Sander, 1993) revealed no structural homologs, and we believe that IF2/eIF5B represents a novel protein fold. Structure-based amino acid sequence alignments of various eukaryotic, archaeal, and eubacterial homologs (Figure 1) demonstrate that conserved residues map to the G domain active site or the hydrophobic cores of each of the four globular domains comprising IF2/eIF5B, whereas insertions and deletions correspond to surface loops. We conclude, therefore, that the phylogenetically conserved core regions of all known IF2/eIF5B homologs share the three-dimensional structure illustrated in Figure 2.

The G domain (residues 1–225) shows significant structural similarity to $p21^{Ras}$, displaying the four conserved sequence elements characteristic of GTP binding proteins (Figure 1; G1/P loop, G2, G3, and G4) (Brock et al., 1998; Lee et al., 1999). In IF2/eIF5B, the G domain is an eight-stranded β sheet of mixed polarity (seven parallel and one antiparallel β strands) flanked by six α helices and a single 3_{10} helix with overall dimensions of 40 Å × 23 Å × 34 Å. Secondary structural elements are arranged in order S1–H1–S2–S3–H2–H3–S4–S5–H4–S6–H5–H6–S7–S8–H7 within the primary sequence. The overall conformation of the G domain is similar among all three of our crystal structures (pair-wise α-carbon root-mean-square deviations or rmsds = 0.3–0.7 Å), with the exception of a single variable region (Asp76–Ala94) corresponding to the Switch 2 region (Figure 1; see below).

Domain II (residues 231–327) is a β barrel (dimensions 25 Å × 30 Å × 30 Å) consisting of eleven antiparallel β

Table 1. Statistics of the Crystallographic Analysis for IF2/eIF5B·GDP, IF2/eIF5B, and IF2/eIF5B·GDPNP

Structure Determination		Reflections	Completeness (%)	R_{sym} (%)		
MAD analysis (16 sites)	Resolution (Å)	measured/unique	overall/outer shell	overall/outer shell	Phasing Power	
					Ano	Iso
λ1 (0.97884 Å)	22.0–2.3	270,190/38,543	88.9/61.3	4.0/10.8	2.86	1.28
λ2 (0.97905 Å)	22.0–2.3	271,531/38,738	82.5/42.3	4.0/12.3	2.27	
		Overall MAD figure of merit: 0.52				
Refinement						
IF2/eIF5B·GDP		Completeness (%)	R_{sym} (%)			
	Resolution (Å)	overall/outer shell	overall/outer shell	Multiplicity	R factor	Free R factor
Data with $\|F\| > 2\sigma(\|F\|)$	22.0–2.0	97.4/86.4	5.6/15.5	6	0.220	0.265
Rms deviations	Bond lengths: 0.009 Å	Bond angles: 1.5°	Thermal parameters: 1.0 Å²			
IF2/eIF5B						
		Completeness (%)	R_{sym} (%)			
	Resolution (Å)	overall/outer shell	overall/outer shell	Multiplicity	R factor	Free R factor
Data with $\|F\| > 2\sigma(\|F\|)$	22.0–2.2	97.0/92.3	2.3/15.4	4	0.243	0.275
Rms deviations	Bond lengths: 0.009 Å	Bond angles: 1.7°	Thermal parameters: 0.7 Å²			
IF2/eIF5B·GDPNP						
		Completeness (%)	R_{sym} (%)			
	Resolution (Å)	overall/outer shell	overall/outer shell	Multiplicity	R factor	Free R factor
Data with $\|F\| > 2\sigma(\|F\|)$	22.0–2.0	97.4/86.0	6.6/17.1	6	0.231	0.267
Rms deviations	Bond lengths: 0.010 Å	Bond angles: 1.6°	Thermal parameters: 0.9 Å²			

$R_{sym} = \Sigma|I - \langle I\rangle|/\Sigma I$, where I = observed intensity, $\langle I\rangle$ = average intensity obtained from multiple observations of symmetry related reflections. Phasing power = rms ($|F_H|/E$), $|F_H|$ = heavy atom structure factor amplitude, and E = residual lack of closure. Rms bond lengths and rms bond angles are the respective root-mean-square deviations from ideal values. Rms thermal parameter is the root-mean-square deviation between the B values of covalently bonded pairs. Free R factors were calculated with 10% of the data omitted from the structure refinements.

Figure 1. Sequence Alignments of Selected IF2/eIF5B Homologs from Eubacteria, Archaea, and Eukaryotes

Sequence numbering scheme corresponds to *M. therm.* IF2/eIF5B (GenBank Accession Code: gi17482858), with GTP binding motifs (G1, G2, G3, and G4) enclosed in red. Secondary structural elements are denoted as follows: α or 3_{10} helices, cylinders; β strands, arrows; random coil, lines. Gray circles represent portions of the polypeptide chain that were not well resolved in the electron density maps. BLOSUM62 (Henikoff and Henikoff, 1992) sequence similarity is color coded using a gradient from white (<40% identity) to dark green (100% identity).

strands, arranged in order S9–S10–S11–S12–S13–S14–S15–S16–S17–S18–S19 (Figures 1 and 2). Despite relatively low amino acid sequence identities (17%–19%), domain II is structurally similar to the second domains of EF-Tu and EF-G (pair-wise α-carbon rmsds = 2–2.4 Å). Three β strands (S10, S11, and S19) are responsible for interacting with the G domain in the vicinity of Switch 2, where they stabilize the relative orientations of domains I and II. There are no significant structural differences in domain II among our three IF2/eIF5B structures (pair-wise α-carbon rmsds = 0.2–0.3 Å).

Domain II connects through a 17 residue α helix (H8) to domain III (residues 344–445), which consists of a four-stranded parallel β sheet flanked on both sides by two α helices (dimensions 25 Å × 25 Å × 27 Å) with a secondary structural arrangement of S20–H9–S21–H10–S22–H11–S23–H12 (Figures 1 and 2). α helix (H12) packs against the dorsal face of the β sheet, and then continues downward to connect to domain IV. To the best of our knowledge, domain III represents a novel protein fold. The Dali server (Holm and Sander, 1993) revealed a maximum Z score of 6.0, corresponding to a fragment of an unrelated α/β protein (methylmalonyl-CoA mutase, PDB ID code 1req). There are no significant structural differences in domain III among our three IF2/eIF5B structures (pair-wise α-carbon rmsds = 0.3–0.4 Å).

The C-terminal domain (residues 462–550) connects to domain III through a 40 Å long α helix (H12) that forms the stem of the chalice. Domain IV, the base of the chalice, consists of an eight-stranded antiparallel β

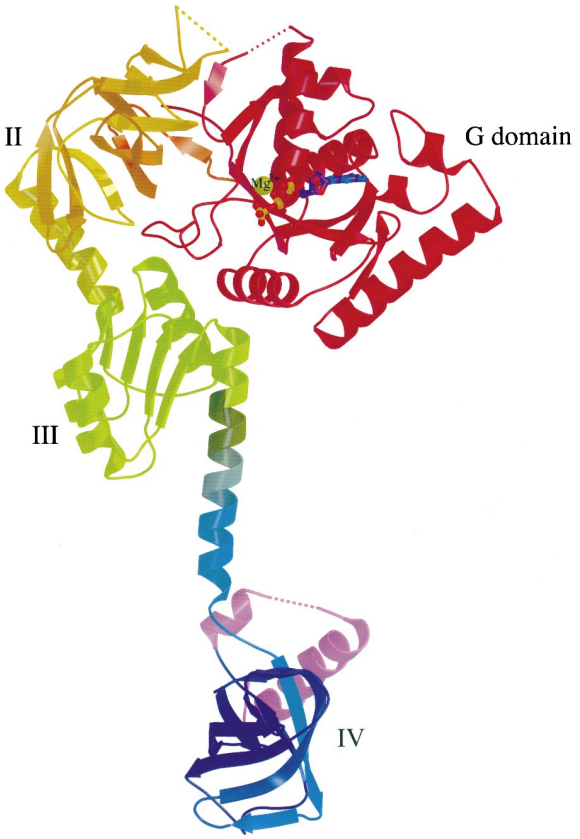

Figure 2. Structure of *M. therm.* IF2/eIF5B·GTP

Ribbons diagram showing the ventral or nucleotide binding site view. Domain color coding is as follows: G domain, red; domain II, yellow; domain III, green; domain IV EF-Tu-type β-barrel, blue; C-terminal α helices, magenta. The bound nucleotide is shown as a ball and stick atomic model, and the Mg^{2+} ion is denoted by a labeled green sphere.

barrel followed by two α helices (dimensions 18 Å × 32 Å × 37 Å) with a secondary structural arrangement of S24–S25–S26–S27–S28–S29–S30–S31–H13–H14 (Figures 1 and 2). The β barrel is structurally similar to domain II of IF2/eIF5B (pair-wise α-carbon rmsd = 1 Å) and to domains II of EF-Tu and EF-G (respective pair-wise α-carbon rmsds = 2.6 and 3.8 Å), despite low amino acid sequence identities (<15%). At the C terminus of IF2/eIF5B, two α helices sit atop the β barrel. α helix H13 packs against the stem α helix (H12) and the short connecting loop that follows. The polypeptide chains for all known eubacterial IF2s end at a point that corresponds to the C terminus of α helix H13. The final secondary structural element, α helix (H14), packs against the dorsal face of the β barrel. The structure of the C-terminal domain of *Bacillus stearothermophilus* IF2 (Meunier et al., 2000) also reveals an EF-Tu-type β barrel, but lacks the two C-terminal α helices (H13 and H14) seen in *M. therm.* IF2/eIF5B. There is no similarity between domains III and IV of IF2/eIF5B and domains III and IV of EF-G. Finally, there are no significant structural differences in domain IV among our three IF2/eIF5B structures (pair-wise α-carbon rmsds = 0.2–0.3 Å).

Comparison with Other GTPases Involved in Protein Synthesis

Figure 3 illustrates the structures of IF2/eIF5B·GDP, EF-G·GDP (Ævarsson et al., 1994), EF-Tu·GDP (Kjeldgaard and Nyborg, 1992), and the EF-Tu·GTP·tRNA ternary complex (Nissen et al., 1995). Residues Gly12–Gly27 of IF2/eIF5B·GDP, forming the P loop and part of α helix H1, superimpose on the corresponding regions of EF-G·GDP and EF-Tu·GDP with pair-wise α-carbon rmsds = 0.3–0.4 Å. In both cases, these structural superpositions result in close overlap of the remaining nucleotide binding segments. Figure 3 also demonstrates that the relative spatial arrangement of the G domain and domain II (the EF-Tu-type β barrel domain) is identical to that seen in the structures of EF-Tu·GTP and EF-G·GDP. It seems likely, therefore, that the N-terminal two domains of the translational GTPases form common structural units that participate in similar interactions with both eukaryotic and bacterial ribosomes.

In all GTPases for which structures of the GDP- and GTP-bound enzymes are available, significant conformational differences are restricted to two polypeptide chain segments, denoted Switch 1 and Switch 2 (Figure 1). Switch 1 is part of the effector region and varies in length and sequence among G proteins, reflecting the fact that this polypeptide chain segment is responsible for interactions with different effector proteins (the ribosome in the case of IF2/eIF5B). Arg33–Ile38 within the effector region could not be resolved in our electron density maps of IF2/eIF5B·GDP, suggesting that it is flexible, as previously seen in EF-G·GDP and EF-Tu·GDP (Kjeldgaard and Nyborg, 1992; Ævarsson et al., 1994; Czworkowski et al., 1994). The Switch 2 region of IF2/eIF5B includes the G2 consensus sequence (Asp–X–X–Gly) and differs substantially in conformation between the GDP- and GTP-bound forms of *M. therm.* IF2/eIF5B (see below).

Guanine Nucleotide Binding to IF2/eIF5B

Guanine nucleotides bind to *E. coli*, human, and *M. therm.* IF2/eIF5B with much lower affinities than to other GTPases (K_d = 1–20 μM). Amino acids involved in nucleotide recognition and binding are largely restricted to four loops connecting secondary structural elements (G1/P loop, G2, G3, and G4; Figures 1 and 4). Two of these loops (G3 and G4) form the walls of a shallow hydrophobic pocket in which the guanine moiety is bound. The P loop between β strand S1 and α helix H1, with consensus sequence Gly–X–X–X–X–Gly–Lys–Thr (Gly12 through Thr19 in *M. therm.* IF2/eIF5B), participates in phosphate binding. In IF2/eIF5B·GDP and IF2/eIF5B·GTP, both the α- and β-phosphate groups are coordinated by the P loop via multiple main chain amide contacts with Gly17, Lys18, Thr19, and Thr20. Not surprisingly, the P loop is disordered in our free enzyme structure of IF2/eIF5B. The Switch 2 region between β strands S4 and S5 contains the Asp–X–X–Gly or G2 motif (Asp76 through Gly79 in *M. therm.* IF2/eIF5B), which is involved in binding of the active site divalent metal.

Magnesium is an essential cofactor for GTP hydrolysis in all G proteins (Kjeldgaard et al., 1996). In IF2/eIF5B·GTP, the catalytic Mg^{2+} ion is situated in a cleft separating the GTP binding site from Switch 2 (Figure

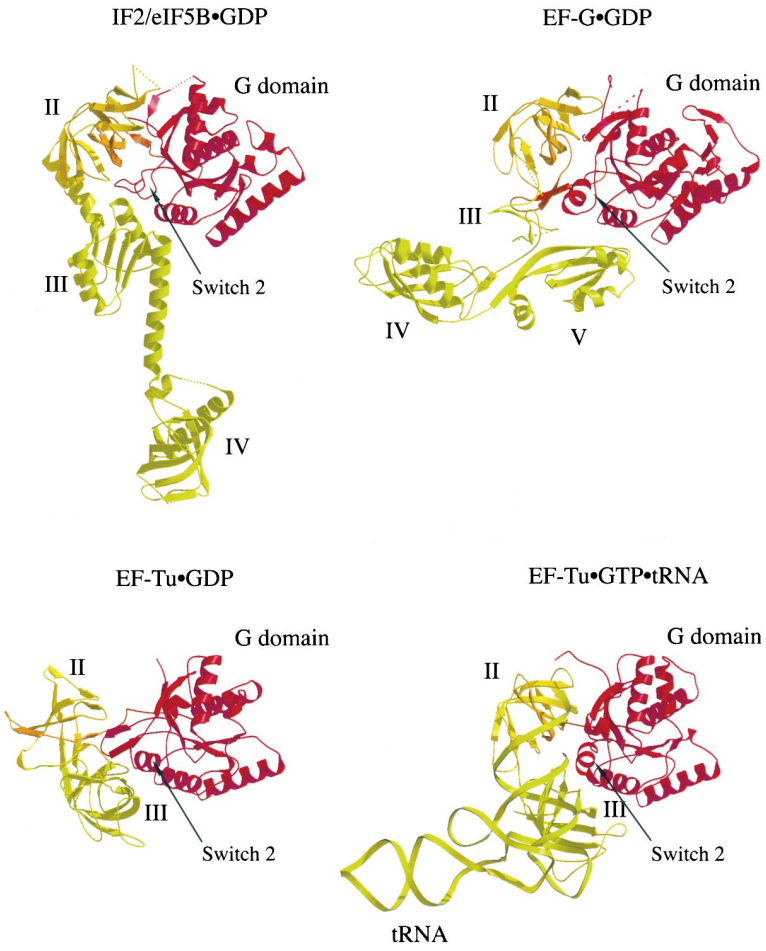

Figure 3. Comparison of Translational GTPase Structures

Ribbon diagrams of IF2/eIF5B·GDP, EF-G·GDP (Ævarsson et al., 1994), EF-Tu·GDP (Kjeldgaard and Nyborg, 1992), and Phe-tRNA^{Phe}·EF-Tu·GDPNP (Nissen et al., 1995). IF2/eIF5B is shown as in Figure 2, with the eubacterial GTPases in the same orientation (based on P loop and α helix H1 structural alignments). Domain color coding: G domain, red; domain II, yellow, domains III and IV of IF2/eIF5B, domains III, IV, and V of EF-G, and domains III of EF-Tu and the Phe-tRNA^{Phe}, light green.

4B), where it is stabilized by direct contacts with the γ- and β-phosphate groups and a P loop hydroxyl group provided by Thr19. Asp76 of G2 (Switch 2) coordinates the divalent cation via a water molecule (Wat1). In both EF-Tu·GTP (Berchtold et al., 1993) and p21^{Ras}·GTP (Pai et al., 1990), the catalytic Mg^{2+} ion is also coordinated by a conserved Thr from the Switch 1/effector region. Contacts between the effector loop and nucleotide or Mg^{2+} are not possible in *M. therm.* IF2/eIF5B·GTP because this region of domain I cannot reach the nucleotide binding site.

The γ-phosphate in IF2/eIF5B·GTP forms a salt bridge with the ε-amino group of invariant Lys18, and is hydrogen bonded to the main chain amide of Asp15 in the P loop (Figure 4B). The sidechains of His80 and Glu81 and a well-ordered water molecule (Wat2) further stabilize the γ-phosphate (Figure 4B). Site-directed mutagenesis of the invariant residue corresponding to His80 in *E. coli* IF2 (His448) and human IF2/eIF5B (His706) substantially affects GTP hydrolysis in both cases. *E. coli* IF2 (His448→Glu) produces in vitro defects in GTP hydrolysis and factor release following ribosomal subunit joining and a dominant-negative effect on growth in vivo (Luchin et al., 1999). Human IF2/eIF5B(His706→Gln) demonstrates a severe reduction in translational stimulatory activity in vitro (assayed with yeast cytoplasmic extract). The His706→Glu mutation has even more striking consequences. This mutant enzyme is inactive in vitro (using the same yeast cytoplasmic extract assay system) and cannot suppress the severe slow-growth phenotype of the *fun12*Δ yeast strain in vivo (Lee et al., 1999).

Conformational Changes in Switch 2 on GTP Binding

We now examine the effects of GTP binding on the Switch 2 conformation by comparing the structures of IF2/eIF5B·GDP and IF2/eIF5B·GTP. Switch 2 is comprised of residues 76–94 and contains the Asp–X–X–Gly G2 consensus sequence, which is invariant among all known IF2/eIF5Bs (Asp–Thr–Pro–Gly). In IF2/eIF5B, Switch 2 makes a significant number of contacts with GTP and Mg^{2+}, but not with GDP. The electron density for the first six residues of Switch 2 in IF2/eIF5B·GDP is rather poor, suggesting that this region is less well ordered in the absence of the γ-phosphate and the divalent cation (residues in Switch 2 have temperature factors higher than the G domain average, 38 Å^2 versus 30 Å^2). Switch 2 is much better defined in IF2/eIF5B·GTP (Switch 2 average temperature factor = 22 Å^2, versus an average of 30 Å^2 for the entire G domain).

Stabilization of Switch 2 when bound GDP is exchanged for GTP is accompanied by a marked conformational rearrangement that can be attributed to the presence of the γ-phosphate and the magnesium ion

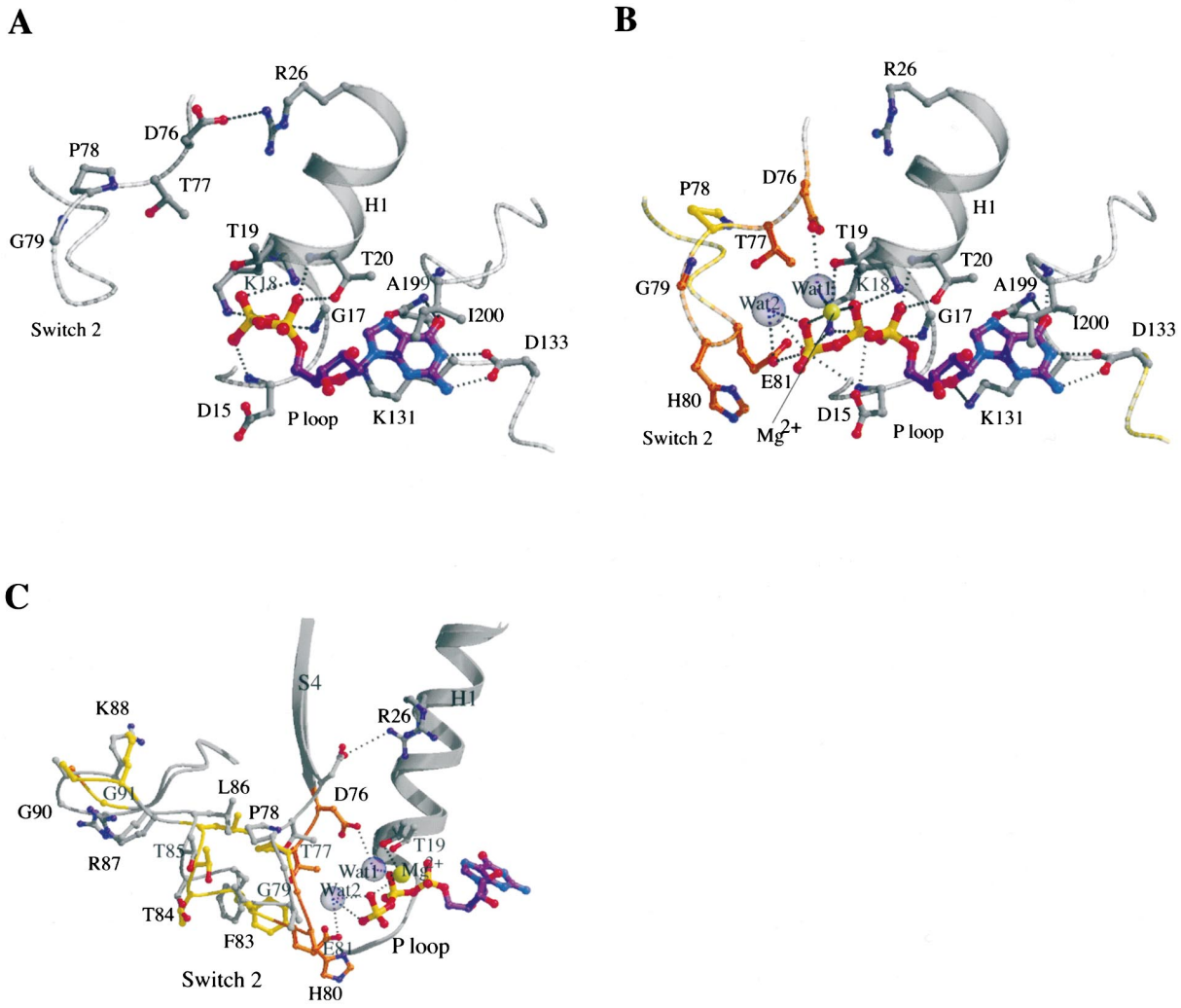

Figure 4. IF2/eIF5B Nucleotide Binding

(A) IF2/eIF5B·GDP showing protein backbone (gray) and ball and stick figure side chains (carbon, gray; oxygen, red; nitrogen, blue) and nucleotide (atomic ball and stick figure). Black dashed lines indicate hydrogen bonds.

(B) IF2/eIF5B·GTP (same view as in A) with protein backbone and side chain carbon atoms color coded for movement of α-carbon atoms relative to the GDP bound structure (<1 Å, gray; 1–2 Å, yellow; 2–3 Å, light orange; 3–4 Å, dark orange; >4 Å, red) Blue spheres represent well ordered water molecules (labeled Wat1 and Wat2), with the Mg^{2+} ion shown in green.

(C) Superposition of the nucleotide binding sites of IF2/eIF5B·GDP and IF2/eIF5B·GTP showing conformational changes in the Switch 2 region induced by GTP/Mg^{2+} binding (same view and color coding as in A and B).

(Figure 4). Upon binding the nonhydrolyzable GTP analog, invariant Asp76 in Switch 2 moves 2.3 Å to form a hydrogen bond with a water molecule (Wat1), that in turn coordinates the Mg^{2+} ion (Figure 4C). Downward movement of Asp76 on GTP binding triggers a conformational change extending throughout Switch 2, which adopts an L-shaped structure starting at Asp76 of G2 and initially running parallel to β strand S1. Thereafter, the polypeptide chain makes a sharp turn at His80 toward the dorsum of the molecule continuing as a short helical turn (residues 82–86) followed by a loop (residues 86–91) that runs almost perpendicular to the Asp–Thr–Pro–Gly motif ending at the dorsal face of the molecule. When GTP binds, Switch 2 moves down and toward the ventral face of the molecule by an average of 2 Å, with a maximal movement of 2.9 Å (conserved Gly90; Figure 4C). Significant G domain conformational changes do not extend beyond Gly91.

In EF-Tu, Switch 2 undergoes a much more profound conformational change on GTP binding (Figure 3, lower panels) (Berchtold et al., 1993). The C terminus of a ten-residue α helix moves 7.5 Å, when conserved Gly84 of the Asp–X–X–Gly Switch2/G2 motif disengages from Asp87 (to which it is hydrogen bonded in EF-Tu·GDP) to interact with the γ-phosphate. (An analogous Gly contributes to nucleotide-induced conformational changes in $p21^{Ras}$ [Kjeldgaard and Nyborg, 1992]). In IF2/eIF5B·GTP, the equivalent glycine (Gly79) is 7.4 Å from the nearest γ-phosphate oxygen atom, effectively precluding direct contact with GTP (Figure 4B).

Amplification of GTP Binding Effects via Coupled Domain Movements

The G domain and domains II and III constitute a single large globular unit, while domain IV, with the long con-

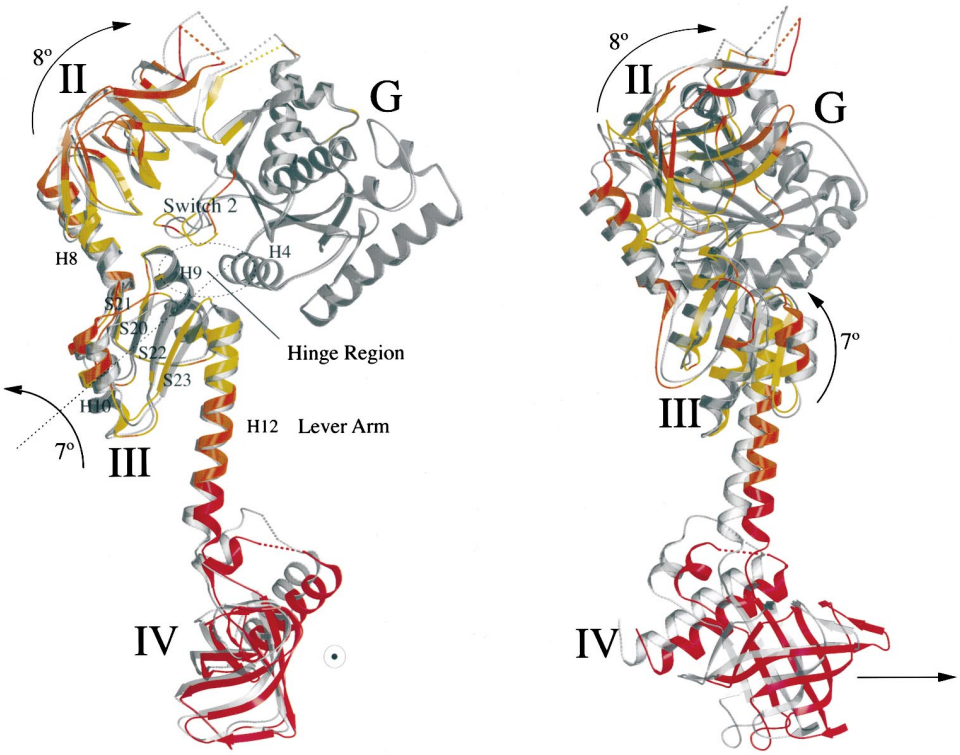

Figure 5. Domain Movements Induced by GTP/Mg^{2+} Binding

Orthogonal views (left, as in Figure 2; right, rotated by 90° about the vertical) of a G domain superposition of IF2/eIF5B·GDP (gray) and IF2/eIF5B·GTP (color-coded as in Figure 4B). Domains are labeled and their relative movements are indicated with arrows. The target symbol denotes movement out of the page.

necting α helix H12, resembles a pendulum with the α helix forming the rod and domain IV the bob. Domain III is quasispherical, and appears to be positioned so as to allow movement of the C-terminal domain. Comparison of the active and inactive states of IF2/eIF5B reveals en bloc repositioning of domains II and III relative to the G domain, coupled to a swinging movement of domain IV of ~4.6 Å on GTP binding (Figure 5).

Switch 2 occupies the "heart" of IF2/eIF5B, surrounded by the G domain and domains II and III, where it is also partially accessible to solvent (Figure 5). In EF-G, Switch 2 is also positioned in the middle of the enzyme, where it mediates contacts between the G domain and domains II, III, and V (Figure 3). In both cases, the central location of Switch 2 allows conformational changes in Switch 2 to be relayed to regions outside the confines of the G domain (Figures 3 and 5). In IF2/eIF5B, the bulk of the Switch 2 region is found at the interface between domains I and II, where 1900 $Å^2$ of solvent-accessible surface area is buried. (The amount of surface area buried at the domain I-II interface does not differ significantly between IF2/eIF5B·GDP and IF2/eIF5B·GTP.)

When IF2/eIF5B binds GTP and Switch 2 undergoes the conformational change depicted in Figure 4C, domain II rotates 8° toward the G domain and moves slightly toward the ventral face of the molecule (Figure 5). Three residues play critical roles at the domain I-II interface (Figures 6A and 6B), including invariant Pro78 in Switch 2, and Leu237 and Glu238 in β strand S10 of domain II. When the GTP analog binds to IF2/eIF5B, Pro78 moves toward the base of the molecule by about 1.3 Å, making more intimate van der Waals contacts with Leu237. The conserved hydrophobic residue Leu237 (Leu, Ile, or Met in all extant IF2/eIF5Bs) makes van der Waals contacts with the N terminus and middle of Switch 2. In IF2/eIF5B·GTP, Pro78 makes additional van der Waals contacts with the side chain of invariant Glu238, which are not observed in IF2/eIF5B·GDP. In the absence of either nucleotide, the electron density for Pro78 is poorly resolved, suggesting that it may exist in multiple conformations in the free enzyme.

Movement of domain II is transmitted to domain III through H8, the domain II-III linker (Figure 5). Like domain II, domain III moves as a rigid body, pivoting about a stable contact point (or "hinge region") between α helix H9 and α helix H4 of the G domain. The position of α helix H4 does not vary between IF2/eIF5B·GDP and IF2/eIF5B·GTP, effectively limiting the motion of domain III to a modest rotation about an axis extending from the H4-H9 interface, through a point between β strands S20 and S22 culminating in the middle of α helix H10 (Figure 5). On GTP binding, domain III rotates 7° toward the dorsal direction, moving the C terminus of β strand S21 backward and the N terminus of β strand S23 forward (Figure 5). Not surprisingly, α helix H9 contains the longest stretch of invariant residues outside the G domain, indicating that this interface with the G domain is functionally important. The medial face of α helix H4 is also conserved among known IF2/eIF5Bs.

The loop between β strand S23 and the long α helix H12 connecting domains III and IV is tethered to the G

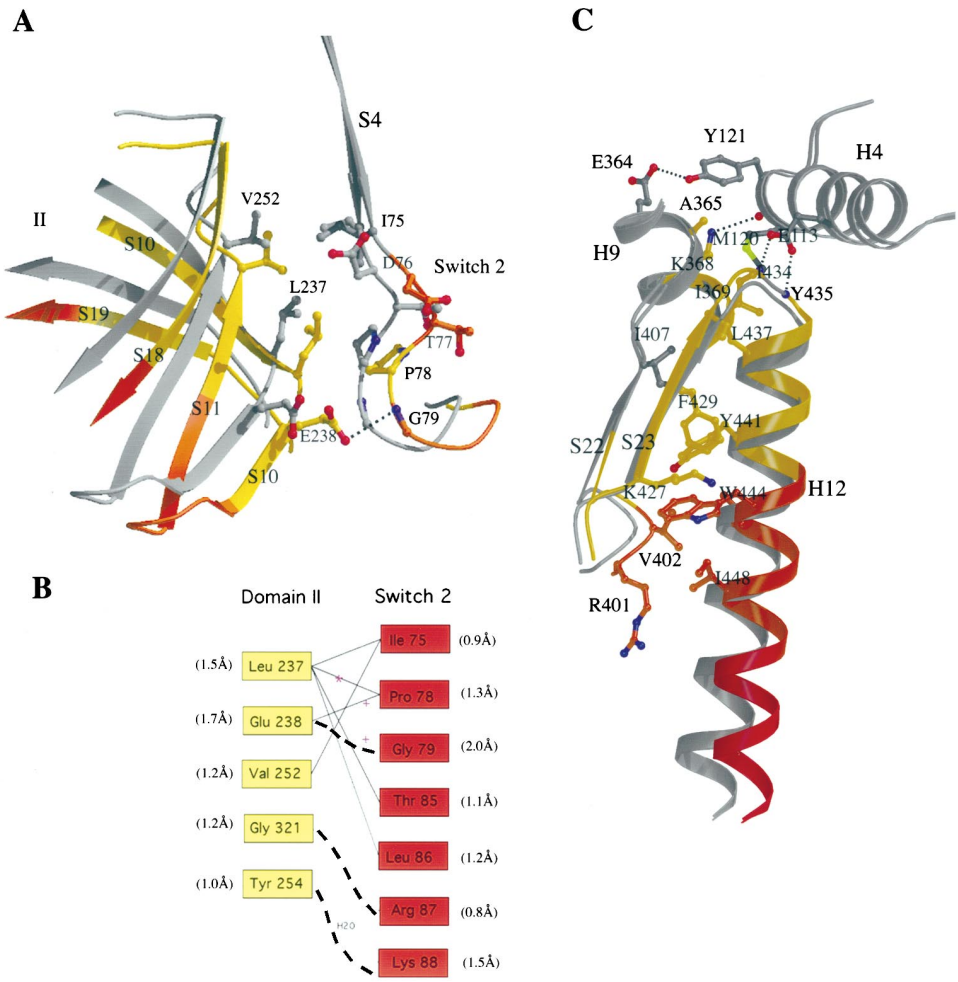

Figure 6. Detailed Comparisons of IF2/eIF5B·GDP and IF2/eIF5B·GTP

(A) Superposition of the interface between Switch 2 and domain II for IF2/eIF5B·GDP (gray) and IF2/eIF5B·GTP (color-coded as in Figure 4B).

(B) Schematic representation of interactions between the Switch 2 region of the G domain (red) and domain II (yellow), showing van der Waals contacts (solid lines) and polar interactions (dashed lines). α-carbon movements between the GDP and GTP bound forms are shown in parentheses for each residue. The symbols "*" and "+"indicate contacts that are weakened or lost, respectively, in IF2/eIF5B·GDP. H_2O denotes an intervening water molecule.

(C) Superposition showing the hinge and arm (α helix H12) regions of the articulated molecular lever (IF2/eIF5B·GDP versus IF2/eIF5B·GTP, colored as in [A]).

domain via hydrogen bonds with residues in α helix H4. The most important interdomain contact residue appears to be invariant Glu113, which makes two hydrogen bonds with the backbone amides of conserved residues Ile434 and Tyr435 (Figure 6C). Mutation of Glu413 in *S. cerevisiae* IF2/eIF5B (corresponding to Glu113 in *M. therm.* IF2/eIF5B) to Asp or Ala has no effect on IF2/eIF5B function in vivo, but a Glu413→Gln substitution inactivates the yeast protein (data not shown). These data suggest that a cavity can be tolerated at this interdomain interface, whereas creation of a bad steric clash between the side chain amino group of the Gln and the backbone amide at the N terminus of α helix H12 destabilizes the structure of IF2/eIF5B.

The movement of domain III is transmitted to domain IV through a 40 Å long lever arm (α helix H12), which pivots about the domain I-III hinge region composed of α helices H4 and H9 (Figure 5). The long lever arm allows amplification of a small movement at the N terminus of α helix H12. A displacement of about 1 Å at the top of domain III translates into a movement of ~4.6 Å at the base of the chalice. α helix H12 swings as a rigid rod toward the ventral plane of the molecule. At its N terminus, α helix H12 contributes to the hydrophobic core of domain III, making conserved hydrophobic contacts with β strands S22 and S23 (Figure 6C). Beyond residue 449, the surface of α helix H12 is exposed to solvent and consists of a stretch of charged residues (Glu–Glu–Glu–Lys–Lys–Lys–Lys). The short linker region connecting α helix H12 to domain IV contains conserved hydrophobic residues that contribute to a series of tight interactions with the surface of domain IV. As a result, this C-terminal domain of IF2/eIF5B moves as a rigid body coupled to domain III (pair-wise α-carbon rmsd =

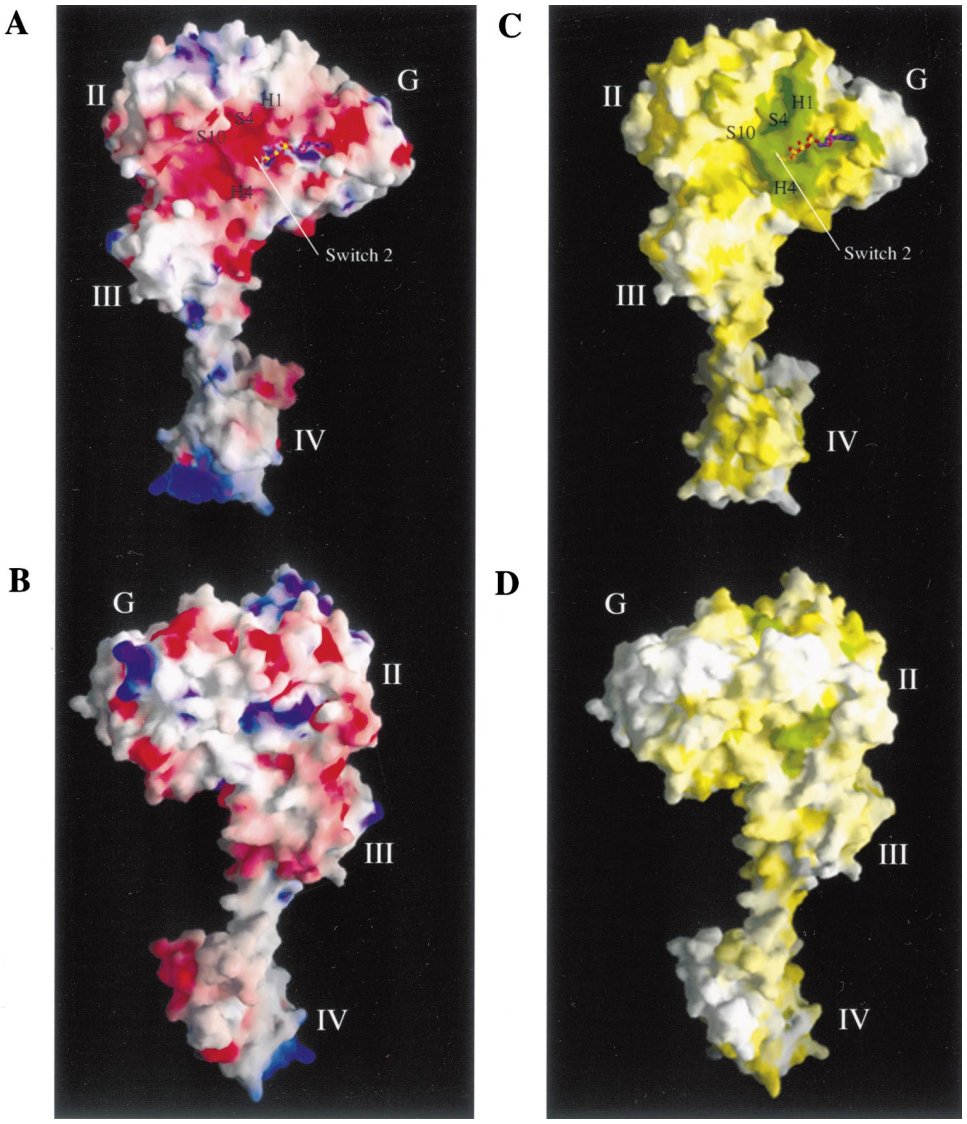

Figure 7. Surface Properties of *M. therm.* IF2/eIF5B

GRASP (Nicholls et al., 1991) representations of the solvent-accessible surface of IF2/eIF5B calculated using a water probe radius of 1.4 Å. Surface electrostatic potential is colored red and blue, denoting less than −15 and greater than +15k_BT, respectively, where k_B is the Boltzmann constant and T is the temperature. The calculations were performed with an ionic strength of 0 mM NaCl and dielectric constants of 80 and 2 for solvent and protein, respectively (Gilson et al., 1988). GTP is shown as a ball and stick figure.

Ventral (A) and dorsal (B) surfaces of IF2/eIF5B·GTP, color-coded for electrostatic potential.

Ventral (C) and dorsal (D) surfaces of IF2/eIF5B·GTP, color-coded for amino acid sequence similarity as in Figure 1.

1.2 Å between GDP- and GTP-bound forms) through the long lever arm α helix H12.

In the absence of a second copy of IF2/eIF5B in the crystallographic asymmetric unit, we cannot rigorously assess the effects of lattice packing interactions on the architecture of this multidomain protein. We are, however, confident that the observed domain movements are not an artifact of crystal packing, because lattice contacts do not vary significantly among our three enzymatic forms of the structure (i.e., free, GDP-, and GTP-bound). Intermolecular interactions within the crystals are modest, including contacts between domain IV and three residues in domain III and between domain IV and a small number of G domain residues (respective buried surface areas, 228 $Å^2$ and 1390 $Å^2$).

IF2/eIF5B Interactions with tRNA and eIF1A

Domain IV of eubacterial IF2 interacts with fMet-$tRNA^{fMet}$, forming a stable binary complex in solution (Spurio et al., 2000). Despite significant pair-wise amino acid sequence identities among various IF2/eIF5B C termini (typically 25%), we have not been able to detect stable complexes of eukaryotic or archaeal IF2/eIF5Bs bound to Met-$tRNA_i^{Met}$ (data not shown). (Both eukaryotes and archaea possess eIF2, which carries the Met-$tRNA_i^{Met}$ to the ribosome [Kyrpides and Woese, 1998]). We cannot, however, rule out ribosomal stabilization of such interactions, since overexpression of the gene encoding $tRNA_i^{Met}$ partially suppresses the severe slow-growth phenotype of the *fun12*Δ yeast strain (Choi et al., 1998).

It has been proposed that the C-terminal β barrel of

eubacterial IF2 interacts with fMet-tRNA^{fMet} in the same way that domain II of EF-Tu binds the 3′ end of aminoacyl-tRNA (Meunier et al., 2000). Our work shows that eubacterial, archaeal, and eukaryotic homologs of IF2/eIF5B actually possess two copies of an EF-Tu-type β barrel (domains II and IV). We suggest that domain II of IF2/eIF5B constitutes part of the ribosome binding platform, leaving domain IV free to interact with tRNA. It is remarkable that fMet-tRNA^{fMet} binds equally well to both IF2·GDP and IF2·GTP (Spurio et al., 2000). This finding is consistent with our X-ray crystallographic results, which demonstrate that the structure of domain IV is not affected by nucleotide binding.

Like members of the IF2/eIF5B family, eubacterial IF1 and eIF1As from archaea and eukaryotes are conserved among all three kingdoms of life (Choi et al., 2000). (Solution NMR studies have demonstrated that *E. coli* IF1 and human eIF1A share a common OB-fold domain [Sette et al., 1997; Battiste et al., 2000]). Eubacterial IF2 and IF1 interact with one another in the presence of the ribosome (Boileau et al., 1983). *S. cerevisiae* eIF1A interacts directly with domain IV of yeast IF2/eIF5B, even in the absence of the ribosome (Choi et al., 2000). Figure 7 illustrates the electrostatic properties (Nicholls et al., 1991) and conservation of surface residues of IF2/eIF5B. Conserved residues in β strands S26 and S28 map to the ventral surface of domain IV, where they could participate in interactions with eIF1A and/or the small ribosomal subunit (see below). Not surprisingly, domain IV of *S. cerevisiae* IF2/eIF5B is essential for function both in vitro and in vivo (Choi et al., 2000).

Mechanistic Model for IF2/eIF5B Function

Our crystal structures provide a basis for analyzing contacts between IF2/eIF5B and the ribosome. The green color-coded portion of the molecular surface depicted in Figure 7C denotes surface-accessible residues that are conserved among all known IF2/eIF5Bs from eubacteria, archaea, and eukaryotes (Figure 1). An invariant acidic surface feature overlies much of the G domain and part of domain II (Figures 7A and 7C), not unlike the acidic ventral surface of EF-Tu. We believe that this conserved feature on the ventral surface of IF2/eIF5B serves as a ribosome binding site (see below). It is remarkable that the balance of the ventral surface of IF2/eIF5B is also highly conserved (Figure 7C), explaining, at least in part, why human and archaeal IF2/eIF5B homologs suppress the severe slow-growth phenotype of the *fun12*Δ strain of yeast in vivo (Lee et al., 1999). In contrast, the dorsal surface of IF2/eIF5B has not been as well preserved during the course of evolution (Figure 7D), and represents an unlikely binding site for the ribosome or other conserved components of the translation machinery.

Our high-resolution structures of the GDP- and GTP-bound forms of IF2/eIF5B allow us to suggest a mechanism by which this universal translation initiation factor promotes ribosomal subunit joining. Domain IV of IF2/eIF5B interacts with eIF1A (Choi et al., 2000), which would place the C terminus of IF2/eIF5B near the surface of the small subunit in the vicinity of the ribosomal A site. (*E. coli* IF1 binds to the A site of the eubacterial ribosome [Moazed et al., 1995]). The N-terminal half of the core region of IF2/eIF5B interacts with the large ribosomal subunit, allowing the protein to serve as a molecular bridge between the two halves of the ribosome. We presume that this bridging function depends critically on the precise spatial arrangement of the G domain and domain II relative to domains III and IV. This stereochemical requirement could be achieved by Mg^{2+}/GTP binding to IF2/eIF5B, which causes en bloc movements of domains II, III, and IV relative to the G domain (Figure 5). The long α helix (H12) running between the cup and the base of the molecular chalice serves as a connecting arm. The C-terminal half of α helix H12 does not appear to interact specifically with the ribosome, because substitution of residues 851–855 in *S. cerevisiae* IF2/eIF5B (corresponding to residues 449–453 of the *M. therm.* protein) with five residues from α helix H6 has no effect on *S. cerevisiae* IF2/eIF5B function in vivo (data not shown).

IF2/eIF5B and IF1/eIF1A constitute the only translation initiation factors known to be conserved among all three kingdoms of life. It has been proposed that these universal factors serve together as structural mimics of EF-G·GDP and the EF-Tu·GTP·tRNA ternary complex (Brock et al., 1998). The G domain and domain II of IF2/eIF5B are structurally similar to the N-terminal portions of both EF-G and EF-Tu, suggesting that all three proteins can participate in similar interactions with the A site of the ribosome. It is also intriguing that the overall dimensions of IF2/eIF5B are similar to those of EF-G and the EF-Tu·GTP·tRNA ternary complex (Figure 3). Electron microscopic studies have demonstrated that both EF-G and the EF-Tu·GTP·tRNA ternary complex undergo large structural rearrangements during their respective functional cycles (Stark et al., 1997, 2000). The molecular architecture of *M. therm.* IF2/eIF5B appears to be capable of supporting similarly large C-terminal domain excursions. It is possible that GTP hydrolysis by IF2/eIF5B facilitates binding of the EF-Tu·GTP·tRNA ternary complex by leaving a stereochemically appropriate molecular imprint on the surface of the ribosome.

Conclusion

Our high-resolution X-ray structures of three distinct functional states of this highly unusual multi-domain GTPase show that IF2/eIF5B exploits an articulated lever mechanism to transduce the energy of GTP binding from the active site of the N-terminal G domain to a C-terminal EF-Tu-type β barrel over a distance of more than 90 Å. Comparison of active and inactive forms of IF2/eIF5B allowed us to propose a mechanism by which this phylogenetically conserved translation initiation factor facilitates ribosomal subunit joining. Our work also provides a starting point for further crystallographic, biochemical, and genetic studies of IF2/eIF5B and its role(s) in translation initiation. In particular, these results should aid directed, systematic analyses of IF2/eIF5B ribosome binding and GTP hydrolysis, and interactions with IF1/eIF1A and possibly Met-tRNA$_i$.

Experimental Procedures

Protein Preparation and Crystallization

Full-length *M. therm.* IF2/eIF5B (residues 1–594) was expressed in *E. coli* as a GST-fusion protein and purified by affinity chromatography.

Following cleavage with Precision protease, IF2/eIF5B was further purified by ion exchange and gel exclusion chromatography. Free enzyme crystals were grown at room temperature via hanging drop vapor diffusion against 100 mM cacodylate (pH5.8), 18% PEG4000, and 0.2M Li_2SO_4, using a protein concentration of about 15 mg/ml. Crystals of IF2/eIF5B bound to GDP and GDPNP were obtained under similar conditions. The crystals grow in triclinic space group P1 with one protein or protein–nucleotide complex per asymmetric unit for free enzyme (unit cell: $a = 48.31$ Å, $b = 54.35$ Å, $c = 90.98$ Å, $\alpha = 105°$, $\beta = 101°$, $\gamma = 99°$; diffraction limit = 2.2 Å), the GDP- (unit cell: $a = 48.4$ Å, $b = 54.5$ Å, $c = 91.8$ Å, $\alpha = 105°$, $\beta = 100°$, $\gamma = 99°$; diffraction limi t= 2.0 Å), and GDPNP-forms (unit cell: $a = 48.8$ Å, $b = 53.0$ Å, $c = 94.9$ Å, $\alpha = 105°$, $\beta = 95°$, $\gamma = 100°$; diffraction limit = 2.0 Å) of the structure.

Data Collection, Structure Determination, and Refinement

Diffraction data for all three structure determinations were measured at Beamlines X25 and X9B of the National Synchrotron Light Source at Brookhaven National Laboratory. Se-Met MAD data (Hendrickson, 1991) for IF2/eIF5B·GDP were collected at two X-ray wavelengths, corresponding to the white line ($\lambda 1$) and the inflection point ($\lambda 2$) of the Se K-absorption edge. Data were processed using DENZO/SCALEPACK (Otwinowski and Minor, 1997). Sixteen of a possible nineteen Se sites were found using SnB (Weeks and Miller, 1999), followed by anomalous difference Fourier syntheses with preliminary MAD phases. Definitive experimental phases were estimated at 2.3 Å resolution with SHARP (de La Fortelle and Bricogne, 1997), giving a final figure of merit of 0.52 (Table 1). After density modification, 85% of the polypeptide chain could be built into the electron density map using O (Jones et al., 1991). Refinement of the partial model using CNS (Brünger et al., 1998) and calculation of electron density maps with combined phases and later ($2\,|F_{obs}| - |F_{calc}|)\alpha_{model}$ difference Fourier syntheses allowed completion of protein structure building and GDP placement. The current refinement model of IF2/eIF5B·GDP consists of residues 1–33, 38–286, 291–562, and 566–587, plus GDP and 452 water molecules. (Despite the presence of 20 mM $MgCl_2$ in our IF2/eIF5B·GDP crystals, well-ordered Mg^{2+} ions were not detected.) Four regions of the polypeptide chain (residues 34–37, 287–290, 563–565, and 588–594) are not well resolved in the electron density map, and are presumed to be disordered. The working and free R factors for IF2/eIF5B·GDP at 2.0 Å resolution are 22.1% and 26.5%, respectively. PROCHECK (Laskowski et al., 1993) revealed 3/576 unfavorable (ϕ,ψ) combinations, and main chain and side chain structural parameters were consistently better than average (overall G factor = 0.2).

The isomorphous free enzyme structure was refined with CNS using the atomic coordinates of IF2/eIF5B·GDP as a starting model (excluding residues involved in nucleotide binding). After rigid body refinement, alternating cycles of simulated annealing, positional refinement, and model building were employed. The current refinement model of IF2/eIF5B free enzyme consists of residues 1–12, 19–32, 40–79, 82–286, 295–562, and 566–585, plus 264 water molecules. Six regions of the polypeptide chain (13–18, 33–39, 80–81, 287–294, 563–565, and 586–594) are not well resolved in the electron density map and are presumed to be disordered. The working and free R factors for IF2/eIF5B free enzyme at 2.2 Å resolution are 24.3% and 27.5%, respectively, with excellent stereochemistry (overall G factor = 0.2).

The structure of IF2/eIF5B·GDPNP was determined by molecular replacement using the structure of IF2/eIF5B·GDP as a source of independent domain search models (excluding the P loop and the Switch 2 region of the G domain). Difference electron density maps revealed unambiguous density for GDPNP. Several rounds of iterative model building and refinement were performed using O and CNS. The current model consists of residues 1–33, 38–285, 292–558, 566–586, GDPNP, and 338 water molecules. Residues 34–37, 286–291, 559–565, and 587–594 are not well resolved in the electron density map and are presumed disordered. The final model has a working R factor of 23.1% and a free R value of 26.7%, respectively, with excellent stereochemistry (overall G factor = 0.3).

Acknowledgments

At the Brookhaven National Laboratory National Synchrotron Light Source, we thank Drs. H. A. Lewis and L. Berman for access to Beamline X25, and Dr. K. R. Rajashankar for help using Beamline X9B. We thank Dr. J. Bonanno for his invaluable assistance with X-ray measurements, and Drs. L. Bellsolel, G. Blobel, B. Chait, X. C. Chen, R. C. Deo, C. U. T. Hellen, G. A. Petsko, D. Jeruzalmi, J. Kuriyan, C. Kielkopf, R. MacKinnon, S. K. Nair, T. V. Pestova, J. C. Padovan, and K. R. Rajashankar for many useful discussions. We thank H. Chen and G. He for technical help, and T. Niven for editorial assistance. We are grateful to K. L. Remo for providing yeast IF2/eIF5B plasmids, and Dr. J. N. Reeve for the gift of *M. therm.* genomic DNA. S. K. B. is an Investigator in the Howard Hughes Medical Institute. This work was supported by NIH grant GM61262 (to S. K. B.). A. R.-M. was supported by a National Science Foundation Graduate Fellowship and a Burroughs-Wellcome Fund Interfaces Training Grant to The Rockefeller University.

Received August 15, 2000; revised October 2, 2000.

References

Ævarsson, A., Brazhnikov, E., Garber, M., Zheltonosova, J., Chirgadze, Y., Al-Karadaghi, S., Svensson, L.A., and Liljas, A. (1994). Three-dimensional structure of the ribosomal translocase: elongation factor G from Thermus thermophilus. EMBO J. *13*, 1669–1677.

Battiste, J.L., Pestova, T.V., Hellen, C.U.T., and Wagner, G. (2000). The eIF1A solution structure reveals a large RNA-binding surface important for scanning function. Mol. Cell *5*, 109–119.

Berchtold, H., Reshetnikova, L., Reiser, C.O., Schirmer, N.K., Sprinzl, M., and Hilgenfeld, R. (1993). Crystal structure of active elongation factor Tu reveals major domain rearrangements. Nature *365*, 126–132.

Boileau, G., Butler, P., Hershey, J.W., and Traut, R.R. (1983). Direct cross-links between initiation factors *1*, *2*, and *3* and ribosomal proteins promoted by 2-iminothiolane. Biochemistry *22*, 3162–3170.

Brock, S., Szkaradkiewicz, K., and Sprinzl, M. (1998). Initiation factors of protein biosynthesis in bacteria and their structural relationship to elongation and termination factors. Mol. Microbiol. *29*, 409–417.

Brünger, A.T. (1992). Free R value: a novel statistical quantity for assessing the accuracy of crystal structures. Nature *355*, 472–475.

Brünger, A.T., Adams, P.D., Clore, G.M., Gros, P., Grosse-Kuntsleve, R.W., Jiang, J.-S., Kuszewski, J., Nilges, M., Pannu, N.S., and Read, R.J. (1998). Crystallography and NMR system: a new software system for macromolecular structure determination. Acta Crystallogr. *54*, 905–921.

Carrera, P., Johnstone, O., Nakamura, A., Casanova, J., Jackle, H., and Lasko, P. (2000). VASA mediates translation through interaction with a *Drosophila* yIF2 homolog. Mol. Cell *5*, 181–187.

Choi, S.K., Lee, J.H., Zoll, W.L., Merrick, W.C., and Dever, T.E. (1998). Promotion of met-tRNAiMet binding to ribosomes by yIF2, a bacterial IF2 homolog in yeast. Science *280*, 1757–1760.

Choi, S.K., Olsen, D.S., Roll-Mecak, A., Martung, A., Remo, K.L., Burley, S.K., Hinnebusch, A.G., and Dever, T.E. (2000). Physical and functional interaction between the eukaryotic orthologs of prokaryotic translation initiation factors IF1 and IF2. Mol. Cell. Biol. *20*, 7183–7191.

Czworkowski, J., Wang, J., Steitz, T.A., and Moore, P.B. (1994). The crystal structure of elongation factor G complexed with GDP, at 2.7 Å resolution. EMBO J. *13*, 3661–3668.

de La Fortelle, E., and Bricogne, G. (1997). Maximum-likelihood heavy atom parameter refinement for multiple isomorphous replacement and multiwavelength anomalous diffraction methods. In Methods of Enzymology, J. Charles, W. Carter, and R.M. Sweet, eds. (Academic Press: Harcourt Brace Jovanovich), pp. 472–494.

Gilson, M., Sharp, K., and Honig, B. (1988). Calculating the electrostatic potential of molecules in solution: method and error assessment. J. Comput. Chem. *9*, 327–335.

Gualerzi, C.O., and Pon, C.L. (1990). Initiation of mRNA translation in prokaryotes. Biochemistry *29*, 5881–5889.

Hendrickson, W. (1991). Determination of macromolecular struc-

tures from anomalous diffraction of synchrotron radiation. Science *254*, 51–58.

Henikoff, S., and Henikoff, J.G. (1992). Amino acid substitution matrices from protein blocks. Proc. Natl. Acad. Sci. USA *89*, 10915–10919.

Holm, L., and Sander, C. (1993). Families of structurally similar proteins, version 1.0. J. Mol. Biol. *233*, 123–138.

Jones, T.A., Zou, J.Y., Cowan, S.W., and Kjeldgaard, M. (1991). Improved methods for building protein models in electron density maps and the location of errors in these models. Acta Crystallogr. *A47*, 110–119.

Kjeldgaard, M., and Nyborg, J. (1992). Refined structure of elongation factor EF-Tu from Escherichia coli. J. Mol. Biol. *223*, 721–742.

Kjeldgaard, M., Nyborg, J., and Clark, B.F. (1996). The GTP binding motif: variations on a theme. FASEB J. *10*, 1347–1368.

Kolakofsky, D., Ohta, T., and Thach, R.E. (1968). Junction of the 50S ribosomal subunit with the 30S initiation complex. Nature *220*, 244–247.

Kyrpides, N.C., and Woese, C.R. (1998). Archaeal translation initiation revisited: the initiation factor 2 and eukaryotic initiation factor 2B alpha-beta-gamma subunit families. Proc. Natl. Acad. Sci. USA *95*, 3726–3730.

Laalami, S., Putzer, H., Plumbridge, J.A., and Grunberg-Manago, M. (1991). A severely truncated form of translational initiation factor 2 supports growth of Escherichia coli. J. Mol. Biol. *220*, 335–349.

Laskowski, R.J., MacArthur, M.W., Moss, D.S., and Thornton, J.M. (1993). PROCHECK: a program to check stereochemical quality of protein structures. J. Appl. Crystallogr. *26*, 283–290.

Lee, J.H., Choi, S.K., Roll-Mecak, A., Burley, S.K., and Dever, T.E. (1999). Universal conservation in translation initiation revealed by human and archaeal homologs of bacterial translation initiation factor IF2. Proc. Natl. Acad. Sci. USA *96*, 4342–4347.

Luchin, S., Putzer, H., Hershey, J.W., Cenatiempo, Y., Grunberg-Manago, M., and Laalami, S. (1999). In vitro study of two dominant inhibitory GTPase mutants of Escherichia coli translation initiation factor IF2. Direct evidence that GTP hydrolysis is necessary for factor recycling. J. Biol. Chem. *274*, 6074–6079.

Meunier, S., Spurio, R., Czisch, M., Wechselberger, R., Guenneugues, M., Gualerzi, C.O., and Boelens, R. (2000). Structure of the fMet-tRNA(fMet)-binding domain of B. stearothermophilus initiation factor IF2. EMBO J. *19*, 1918–1926.

Moazed, D., Samaha, R.R., Gualerzi, C., and Noller, H.F. (1995). Specific protection of 16S rRNA by translational initiation factors. J. Mol. Biol. *248*, 207–210.

Nicholls, A., Sharp, K.A., and Honig, B. (1991). Protein folding and association: insights from the interfacial and thermodynamic properties of hydrocarbons. Proteins *11*, 281–296.

Nissen, P., Kjeldgaard, M., Thirup, S., Polekhina, G., Reshetnikova, L., Clark, B.F., and Nyborg, J. (1995). Crystal structure of the ternary complex of Phe-tRNAPhe, EF-Tu, and a GTP analog. Science *270*, 1464–1472.

Otwinowski, Z., and Minor, W. (1997). Processing of X-ray diffraction data collected in oscillation mode. Methods Enzymol. *276*, 307–326.

Pai, E.F., Krengel, U., Petsko, G.A., Goody, R.S., Kabsch, W., and Wittinghofer, A. (1990). Refined crystal structure of the triphosphate conformation of H-ras p21 at 1.35 Å resolution: implications for the mechanism of GTP hydrolysis. EMBO J. *9*, 2351–2359.

Pestova, T.V., Lomakin, I.B., Lee, J.H., Choi, S.K., Dever, T.E., and Hellen, C.U. (2000). The joining of ribosomal subunits in eukaryotes requires eIF5B. Nature *403*, 332–335.

Sander, C., and Schneider, R. (1991). Database of homology-derived protein structures and the structural meaning of sequence alignment. Proteins *9*, 56–68.

Sette, M., van Tilborg, P., Spurio, R., Kaptein, R., Paci, M., Gualerzi, C.O., and Boelens, R. (1997). The structure of the translational initiation factor IF1 from E.coli contains an oligomer-binding motif. EMBO J. *16*, 1436–1443.

Spurio, R., Brandi, L., Caserta, E., Pon, C.L., Gualerzi, C.O., Misselwitz, R., Krafft, C., Welfle, K., and Welfle, H. (2000). The C-terminal subdomain (IF2 C-2) contains the entire fMet-tRNA binding site of initiation factor IF2. J. Biol. Chem. *275*, 2447–2454.

Stark, H., Rodnina, M.V., Rinke-Appel, J., Brimacombe, R., Wintermeyer, W., and van Heel, M. (1997). Visualization of elongation factor Tu on the Escherichia coli ribosome. Nature *389*, 403–406.

Stark, H., Rodnina, M.V., Wieden, H.J., van Heel, M., and Wintermeyer, W. (2000). Large-scale movement of elongation factor G and extensive conformational change of the ribosome during translocation. Cell *100*, 301–309.

Weeks, C., and Miller, R. (1999). The design and implementation of SnBv2.0. J. Appl. Crystallogr. *32*, 120–124.

Wilson, S.A., Sieiro-Vazquez, C., Edwards, N.J., Iourin, O., Byles, E.D., Kotsopoulou, E., Adamson, C.S., Kingsman, S.M., Kingsman, A.J., and Martin-Rendon, E. (1999). Cloning and characterization of hIF2, a human homologue of bacterial translation initiation factor *2*, and its interaction with HIV-1 matrix. Biochem. J. *342*, 97–103.

Wu, X.Q., Iyengar, P., and RajBhandary, U.L. (1996). Ribosome-initiator tRNA complex as an intermediate in translation initiation in Escherichia coli revealed by use of mutant initiator tRNAs and specialized ribosomes. EMBO J. *15*, 4734–4739.

Protein Data Bank ID Codes

Atomic coordinates and structure factor amplitudes have been deposited in the Protein Data Bank with ID codes as follows: Free, 1G7R; GDP, 1G7S; GDPNP, 1G7T.